



FEC 2020

28th IAEA Fusion Energy Conference

TERMINATION OF DISCHARGES IN HIGH PERFORMANCE SCENARIOS IN JET

Carlo Sozzi

IAEA-CN-978

JET



This work has been carried out within the framework of the EUROfusion Consortium and has received funding from the Euratom research and training programme 2014-2018 under grant agreement No 633053. The views and opinions expressed herein do not necessarily reflect those of the European Commission.

Author's list



C. SOZZI, E. ALESSI

Istituto per la Scienza e Tecnologia dei Plasmi-Consiglio Nazionale delle Ricerche

Milano, Italia

Email: carlo.sozzi@istp.cnr.it

P.J. LOMAS, F.RIMINI, C.STUART, C. CHALLIS, L. GARZOTTI, M. LENNHOLM*, S. GERASIMOV, C. MAGGI, D. VALCARCEL

United Kingdom Atomic Energy Authority, Culham Centre for Fusion Energy, Culham Science Centre Abingdon, United Kingdom, [*also European Commission, Brussels, Belgium]

J. HOBIRK, A. KAPPATOU

Max Planck Institute for Plasma Physics

Garching, Germany

A.PAU, O.SAUTER, M. FONTANA, G. MARCECA

Swiss Plasma Centre - École polytechnique fédérale de Lausanne

Lausanne, Switzerland

D.R.FERREIRA, I. S.CARVALHO

Instituto de Plasmas e Fusão Nuclear, Instituto Superior Técnico, Universidade de Lisboa

Lisboa, Portugal

S. ALEIFERIS

Institute for Nuclear and Radiological Science and Technology, Safety and Energy, NCSR Demokritos,

Athens, Greece

B. CANNAS, A. FANNI, G. SIAS

Electrical and Electronic Engineering Department, University of Cagliari

Cagliari, Italy.

E. DE LA LUNA

Laboratorio Nacional de Fusión, CIEMAT

Madrid, Spain

D. FRIGIONE, G.PUCELLA, E.GIOVANNOZZI, P.BURATTI

ENEA, Fusion and Nuclear Safety Department, C. R. Frascati, Roma, Italy

E. JOFFRIN

CEA, IRFM

St Paul Les Durance, France

E. LERCHE, D. VAN EESTER

Laboratory for Plasma Physics -École Royale Militaire

Brussel, Belgium

L. PIRON

Dipartimento di Fisica "G. Galilei", Università degli Studi di Padova & Consorzio RFX

Padova, Italy

and JET Contributors

See the author list of 'Overview of JET results for optimising ITER operation' by J. Mailloux et al to be published in Nuclear Fusion Special issue: Overview and Summary Papers from the 28th Fusion Energy Conference (Nice, France, 10-15 May 2021)

1. INTRODUCTION



- The termination of high performance plasmas in tokamak devices with high Z metal plasma facing components presents challenges related to the influx of heavy impurities which, if not kept under control, cause an increase of the radiative losses, radiative cooling and high probability of disruption. The first generation of tokamaks from the end of 50th until middle of 70th had high Z-metal wall, and they suffered with impurity accumulation and high disruption rate [1]. A number of key players in these dynamics have been identified by intensive research performed after the first years of operation in tungsten machines as AUG and JET in preparation of ITER operation. Inward neoclassical convection related to the peaking of the density profile, poloidal asymmetries, plasma rotation and centrifugal effects, temperature screening, pedestal temperature, pedestal density and ELMs control are among them [2][3][4].
- The objective of D-T fuelled plasmas with high neutron yield in stationary conditions, foreseen in the near future at JET, focuses the operations towards high performance in terms of thermal energy content and plasma current and consequently with higher disruption risk. The reduction of such risks has been pursued for the specific features of the two plasma scenarios being developed, baseline ($\beta_N \sim 1.8$, $q_{95} \sim 3$) and hybrid ($\beta_N \sim 2-3$, $q_{95} \sim 4$) [5] during the various phases of the 2019-20 experimental campaign. In 2019-20 the available additional power for scenario development has been higher (PNBI up to 32MW, with >30MW for 3s on a large number of shots) than in the 2016 campaign (PNBI \approx 28MW). The baseline approach mainly develops at high current and field limits with a relaxed current profile ($I_p=3.8-4.5$ MA, $B_T=3.45-3.7$), whereas the hybrid one addresses the advantages of operating at high β_N with a wider current profile and $q_{min}>1$ with lower current and field ($I_p=2.2-2.5/2.5-2.9$ MA, $B_T=2.8-3.4$). In most of hybrid pulses the flat top current I_p is lower than value reached at the end of the ramp-up phase $I_{p,max}$.

2.DISRUPTION RATE IN HIGH BASELINE SCENARIO

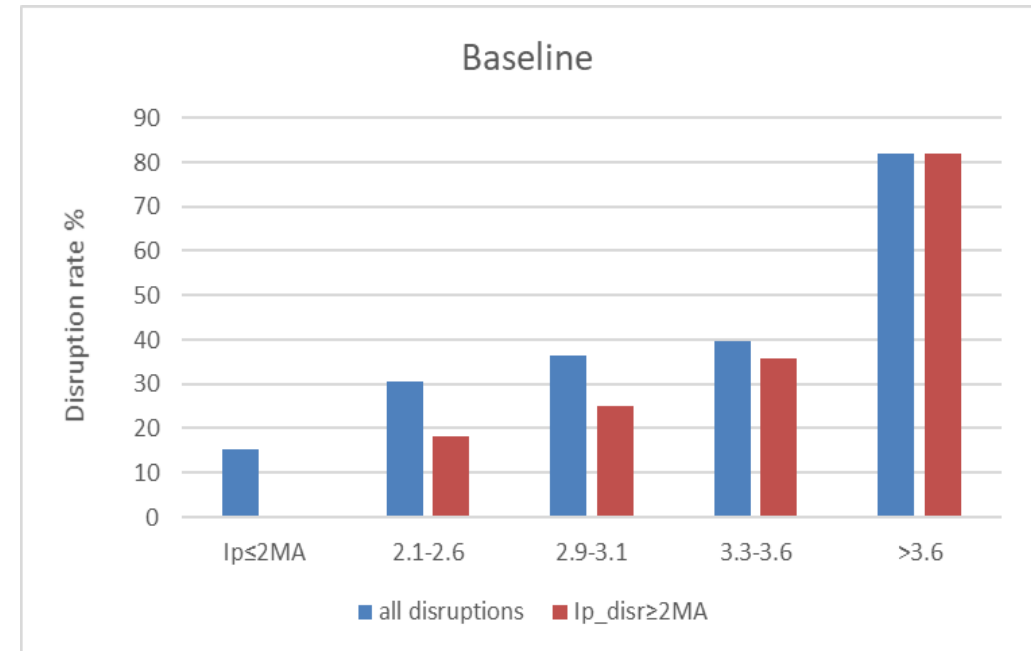


- The high plasma current ($I_p \geq 2.5 \text{ MA}$) experiments based on the baseline scenario performed in the high power campaign in 2016 had 65% overall disruption rate (for $I_{p, \text{disr}} \geq 1.0 \text{ MA}$, where $I_{p, \text{disr}}$ is the plasma current at the time in which the disruption occurs) with 49% pulses ending with the disruption occurring at a plasma current such that a mitigation action is required, i.e. $I_{p, \text{disr}} \geq 2.0 \text{ MA}$ (or total internal energy $\geq 5 \text{ MJ}$).
- The disruption rate is computed as the fraction of the disrupting pulses among the ones reaching the flat top phase or the end of the plasma current ramp-up.
- The inspection of the corresponding databases for the 2019-20 campaign reveals a significant reduction of the disruption rate. The 2019-20 database for baseline scenario development encompasses 390 pulses reaching the flat top phase 339 of which with a flat top phase of at least 1 s. The overall disruption rate is 32% but it is reduced at 21% if only the disruptions at $I_{p, \text{disr}} \geq 2.0 \text{ MA}$ are accounted for. However, the rate of disruption rate increases at high plasma current (3.5-4 MA) i.e. in the range of operational parameters in which the highest fusion performance is expected and therefore is the objective of the development effort.

2.DISRUPTION RATE IN BASELINE SCENARIO



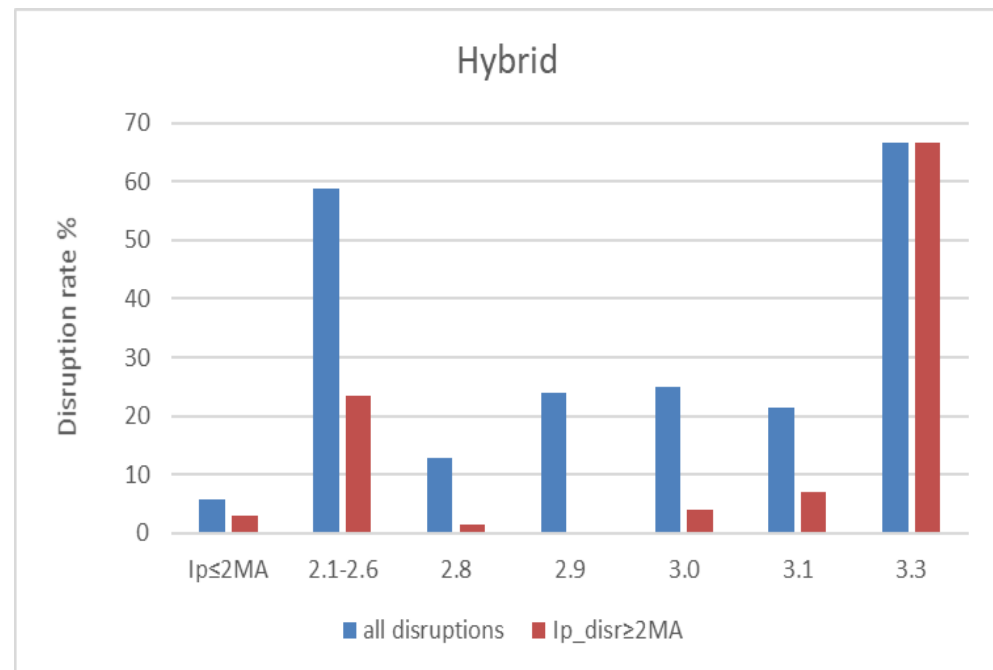
- This is shown in FIG. 1, where the disruption rate is represented for the different values of the flat top plasma current. In the vast majority of the cases the disruption occurs at a lower plasma current with respect to the flat top value, i.e. during the current ramp-down, but still at a current value $I_{p,disr} \geq 2$ MA requiring mitigation according to the JET Operations Instructions.
- The high disruption rate for $I_p > 3.6$ MA also reflects the limited number of attempts to develop the scenario in such range (11 pulses) and the statistical uncertainty.



2.DISRUPTION RATE IN BASELINE SCENARIO



- The overall 2019-20 database for hybrid scenario development encompasses 422 pulses of which 311 reached the flat top phase that lasted for at least 1 s. The overall averaged disruption rate is 20% but the vast majority of disruption occurs at low current (well below the mitigation limit) so that the overall mitigated disruption rate (i.e. for $I_{p,disr} \geq 2$ MA) is about 2%.
- FIG. 2 shows the disruption rate for different intervals of the maximum plasma current. Both the intervals with higher disruption rates correspond to ranges of parameters only marginally explored (17 pulses for $2.1 \leq I_{p,max} \leq 2.6$ MA and 3 for $I_{p,max} \geq 3.3$ MA). The rate of mitigated disruptions is respectively of 3% at $I_{p,max} = 3.0$ MA and 6% at 3.1 MA where respectively 52 and 188 pulses were performed to develop the scenario. It should also be noted that in the hybrid scenario the maximum current is reached at the end of the ramp-up. The flat top value is in most cases maintained in the range of 2.2-2.5 MA.





- A reduced disruptions database for 2019-20 campaign, limited to the cases with either $I_{p,max}$ or $I_p > 2.8$ MA has been studied to identify the sequence of events preceding the disruption. This database includes 88 disruptions for the baseline scenario and 68 for the hybrid. The selected range includes the main development ground for both scenarios, typically $I_p = 3.0-3.6$ MA in flat top for baseline and $I_{p,max} = 2.8-3.1$ in current ramp, $I_p = 2.2-2.5$ in flat top for hybrid.
- The majority of disruptions in the termination of the high performance scenarios in JET are initiated by radiative events either radially located in the plasma core or off axis, often in the low field side.
- Such events drive either the broadening or the shrinking of the current density profile as consequences of the cooling effect on the electron temperature profile, respectively hollowing (TH events) at the core or cooling at the edge (EC events), related with the local enhancement of radiation [7].
- Both broadening and shrinking of the current density are causes of an increased probability the destabilization of the 2/1 tearing mode due to the increased current density gradient in the $q=2$ region. In the case of TH events also the impurity concentration (Z_{eff} profile) plays a role in the same destabilizing direction.



- TH and EC events may occur either alone or in conjunction. Table 1 reports the statistical incidence in the C38 reduced database of such well recognized chain of events.
- It can be seen that TH and EC events precede about 90% of the disruption in baseline scenario and about 80% in the hybrid.
- TH events only precede about 36% of the disruption in baseline and 46% in hybrid.
- One disruption path (NTM in landing) consisting in pacing the RF power in the termination to impose a high enough sawtooth rate to ensure efficient core impurity flushing in the hybrid termination scheme has been optimized along the campaign reducing the risk of NTM triggering after a long sawteeth.
- The evaluation of the disruption rate is partially biased by the fact that part of the disruptions is actually triggered by the JET plasma control system which is set to trigger the Massive Gas Injection system [8] for mitigation when a severe risk of components damage or of a heavy impact on plasma operations is approached. This does not allow to evaluate if in a fraction of cases the plasma without the MGI could have survived.

2.DISRUPTION RATE IN HIGH PERFORMANCE SCENARIOS



Table 1. Statistical incidence of the various disruption paths in 2019-20 campaign

Baseline/Events%	NTM in landing	Temperature Hollowing	Edge Cooling	Both	Other	Ramp-up
94214-96538	0.0	16.7	52.8	27.8	2.8	0.0
96705-96999	0.0	21.1	57.9	21.1	0.0	0.0
97391-97874	8.7	21.7	39.1	8.7	21.7	0.0
97910-98006	10.0	0.0	70.0	10.0	10.0	0.0
Total	3.4	17.0	52.3	19.3	8.0	0.0

Hybrid/Events%	NTM in landing	Temperature Hollowing	Edge Cooling	Both	Other	Ramp-up
94191-96531	9.4	34.4	34.4	0.0	15.6	6.3
96660-97021	5.0	30.0	25.0	30.0	10.0	0.0
97449-97853	0.0	43.8	31.3	12.5	12.5	0.0
97896-97898	0.0	0.0	0.0	0.0	0.0	0.0
Total	5.9	35.3	30.9	11.8	13.2	2.9

3. DISRUPTION AVOIDANCE SCHEMES



- With respect to the typical termination scheme previously adopted the gas fuelling has been increased to boost the ELM frequency in order to favour the impurities removal at the plasma edge and to reduce the divertor temperature[3][4][9]. In pulse 94811 the slower NBI power ramp-down delays the H-L transition.
- An accurate control of the additional power in this phase is essential to avoid or shorten the ELM-free phase at the start of the ramp-down that may inhibit the impurity expulsion by the ELMs. In addition to the reduction in ELM frequency, the problem with ELM free phases is that the impurities penetrate easily during the inter ELM phases given them the opportunity to move above the pedestal where they can not be expelled and then the core transport takes over.
- An increase of the core electron heating can be obtained by increasing the H minority fraction injected during the ramp-down. The two pulses also differ for the percentage of minority gas H₂ injected and for the duration of the ICRH heating waveform.
- In pulse 94811 positive indications of the effectiveness of this combination of settings are visible in the bulk radiation which is kept under control, in the electron temperature profile which remains peaked, and in the n=1 mode activity, which precedes the locked mode phase. The latter leads to the disruption of pulse 94810, while it is avoided in 94811. However, the validity of this scheme in a statistically significant ensemble that may help in disentangling the concurrent factors is still to be proven and its extension at higher plasma current is not yet demonstrated.

3. DISRUPTION AVOIDANCE SCHEMES

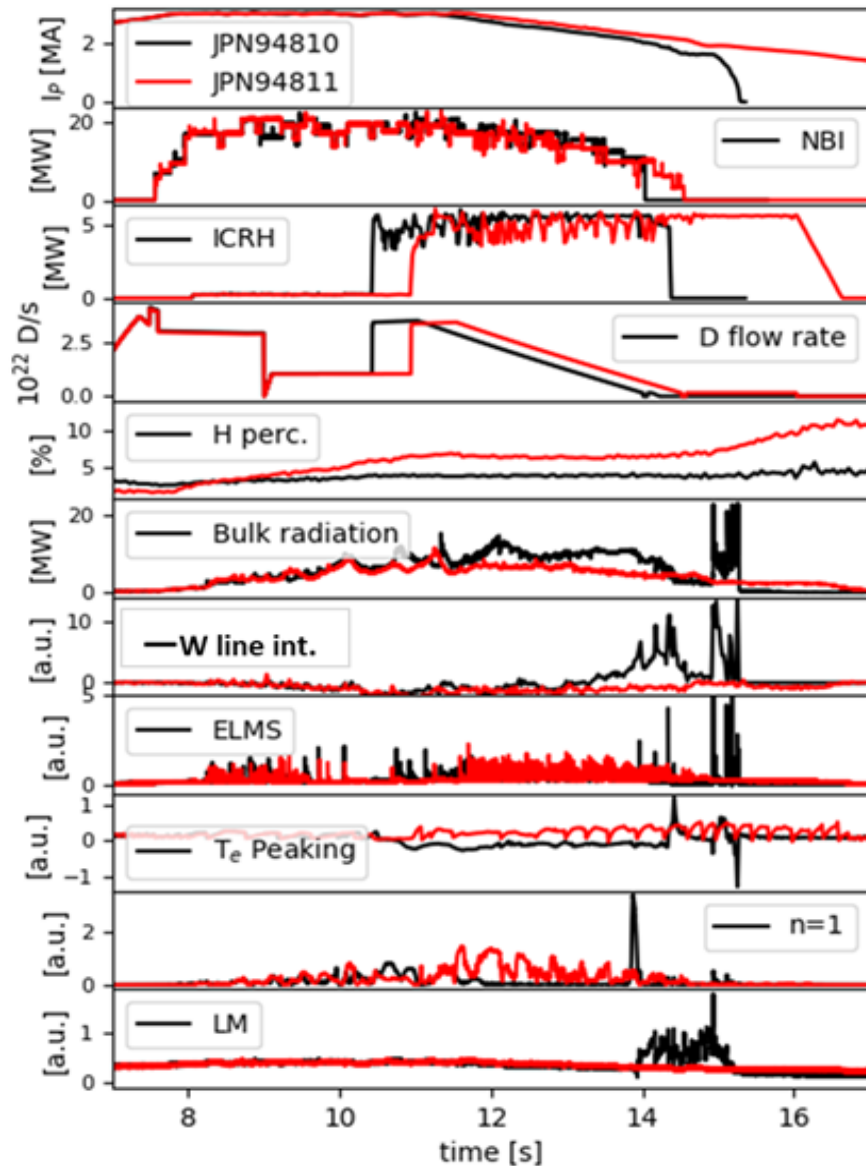


FIG. 3

- In pulse 94811 positive indications of the effectiveness of this combination of settings are visible in the bulk radiation which is kept under control, in the electron temperature profile which remains peaked, and in the $n=1$ mode activity, which precedes the locked mode phase.
- The latter leads to the disruption of pulse 94810, while it is avoided in 94811.
- However, the validity of this scheme in a statistically significant ensemble that may help in disentangling the concurrent factors is still to be proven and its extension at higher plasma current is not yet demonstrated.



4.

REAL-TIME DETECTION OF UNHEALTHY PLASMA CONDITIONS

4.1. Temperature Hollowing and Edge Collapse parameters



- The two parameters defined in [7] to describe the link between temperature profile behaviour and disruption path, the Edge Cooling $EC = \langle T_e \rangle_{V_{mid}} / \langle T_e \rangle_{V_{ext}}$, and the Temperature Hollowing $TH = \langle T_e \rangle_{V_{mid}} / \langle T_e \rangle_{V_{int}}$, where, respectively, V_{int} includes radiometers channels having $3.0m < R_{int} < 3.4m$, V_{mid} with $3.4m < R_{int} < 3.6m$ and V_{ext} with $3.6m < R_{int} < 3.8m$ also may have an operational application as disruption precursors.
- The stable phase of a plasma discharge is associated with a well defined region in the plane of the two parameters EC, TH. During the instable phase preceding the mode lock one or both the parameters cross an empirically established threshold.

4.1. Temperature Hollowing and Edge Collapse parameters

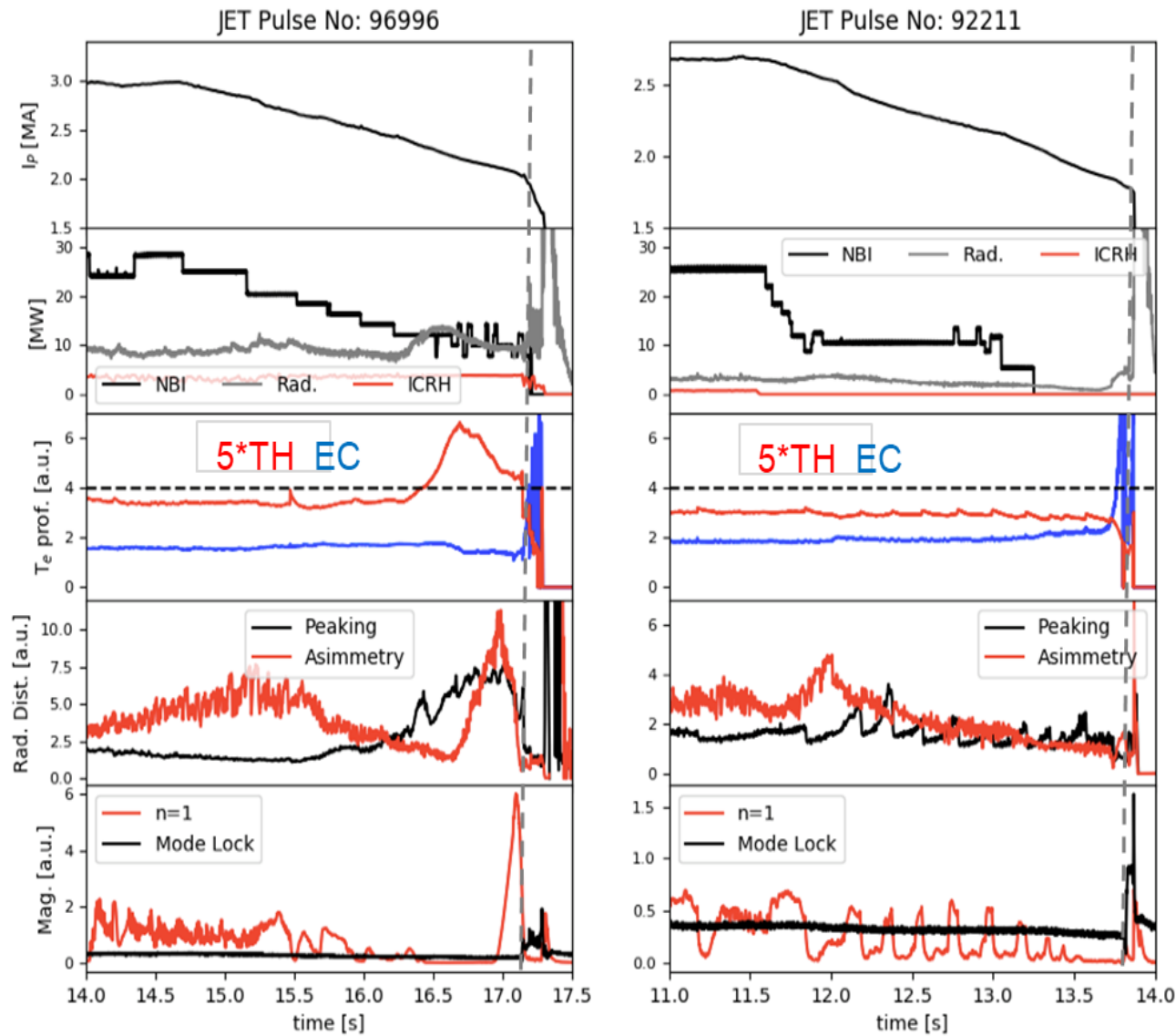


FIG. 4

- Two examples of such behaviour are shown in FIG. 4 . The EC and TH parameters are scaled in the figure in order to have the same threshold value (dashed line).
- In the case of 96996 a nearly simultaneous evolution of the radiation distribution with the TH parameter can be observed. The EC parameters in this pulse increases for minor disruptions only after the onset and locking of the mode.

4.1. Temperature Hollowing and Edge Collapse parameters



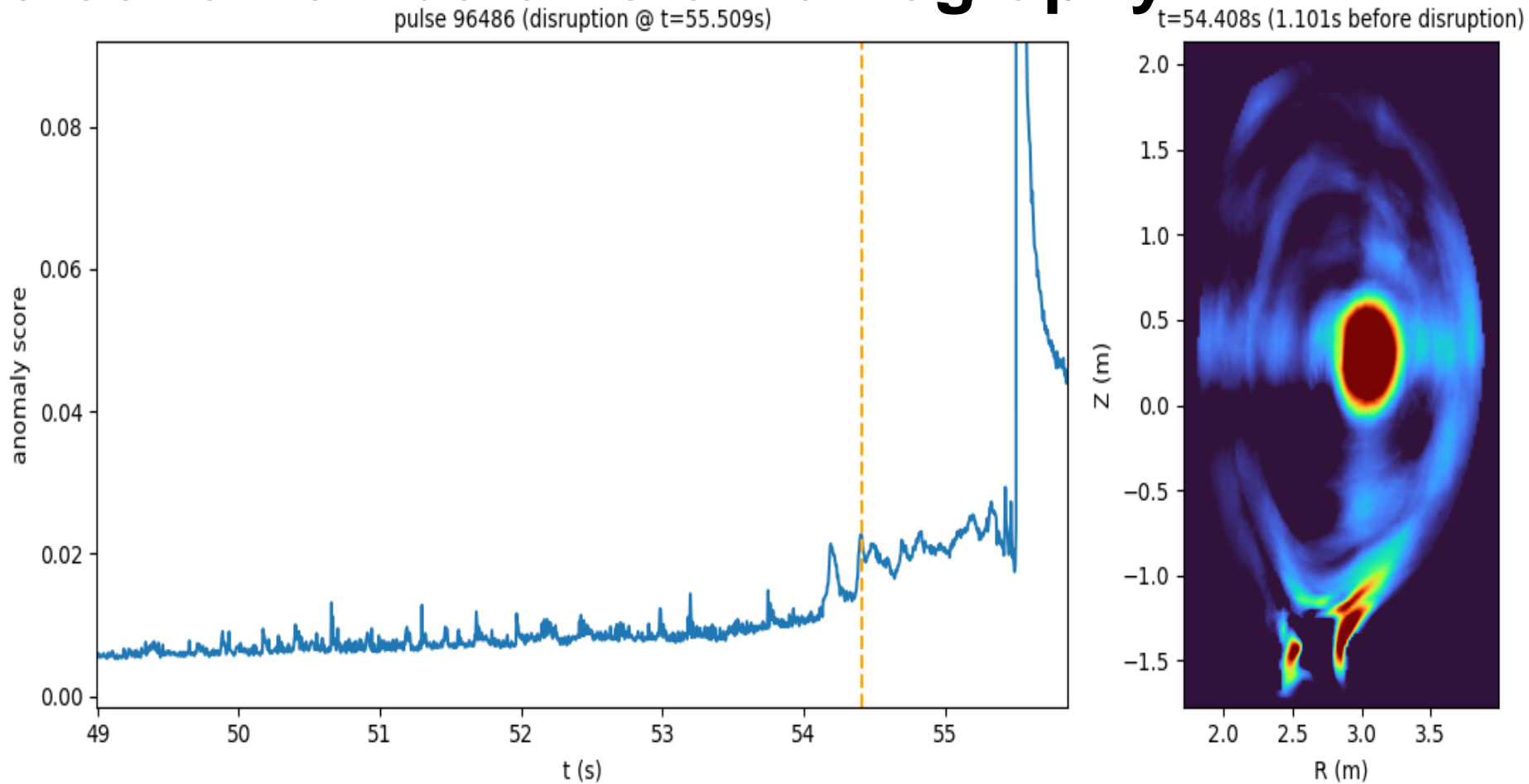
- The distributions of the time interval between the increase of the parameters values and the locked mode in a disruption indicate that TH and EC could provide alerts falling within 2 s and 200 ms respectively before the locked mode. For the time scale of the JET plasmas 2 s are sufficient to trigger a recovery action while 200 ms are sufficient for an early mitigation.

4.2. Real-time reconstruction and anomaly detection on bolometer tomography



- Several improvements on the elaboration of bolometry data for the purpose of disruption avoidance have been implemented, namely a real-time tomography reconstruction which can estimate the amount of radiated power from different regions of interest in the poloidal plane[10]. In particular, this technique makes possible the quantitative evaluation of the poloidal distribution of the radiated power in case of either symmetric or asymmetric radiation allowing to identify the first stages of enhanced core radiation that may help to discriminate a pre-disruptive behaviour.
- More recently, a two-step method has been applied with the purpose of detecting incoming disruptions [11]. A fast tomographic reconstruction method to generate radiation profiles has been implemented based on a matrix multiplication model, trained on existing sample reconstructions. This is being applied to generate the profiles for any given pulse (disruptive or non-disruptive).

4.2. Real-time reconstruction and anomaly detection on bolometer tomography



- On top of reconstruction, an anomaly detector technique to point out unusual profiles has been implemented using a variational autoencoder. Such detector has been trained on profiles from non-disruptive pulses only. When applied on profiles from disruptive pulses, this method provides an anomaly score on each 2-D profile. FIG. 5 shows an example for a disruptive pulse in which the anomaly score starts to increase more than 1 s before the disruption.

4.3. Real time application of ECE interferometry for disruptions avoidance



- The Electron Cyclotron Emission interferometer at JET provides absolutely calibrated real-time temperature profiles with a time resolution of 16 ms (60 Hz) [12].
- This allows to implement simple and robust metrics to characterize the peaking or hollowness of the temperature profiles ($P_1 > 0$, peaked, $P_1 < 0$, hollow) using pre-defined radial windows optimized for the specific real-time application, such as shown in FIG. 6. This has been firstly applied to soft stop and safe early terminating hybrid scenario pulses developing hollow temperature profiles triggering harmful tearing modes during the ramp-up phase [13].

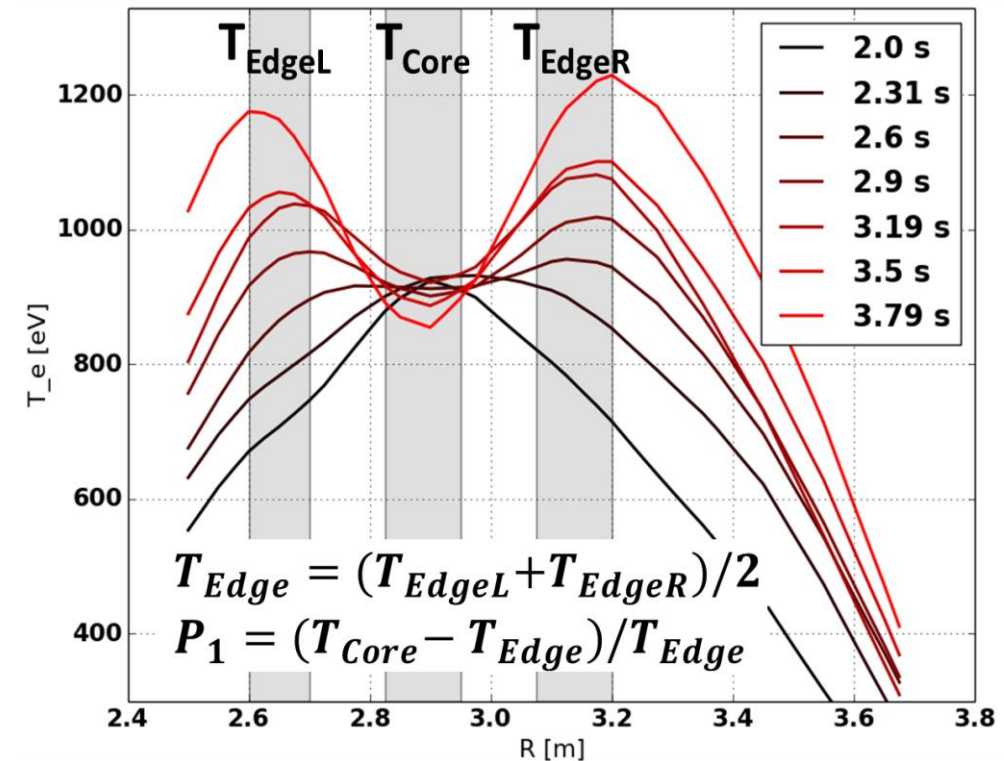


FIG. 6 Radial windows for the P_1 peaking/hollowness temperature metrics

4.3. Real time application of ECE interferometry for disruptions avoidance



- Since also a metric for edge cooling based on the edge temperature gradient can be defined using the interferometry data a second interesting application concerns the detection of unhealthy plasma conditions in the termination.
- Applied on a sub-set of 53 baseline discharges, the combination of the peaking and gradient parameters has shown interesting potential for early disruption detection with a warning time of few hundreds ms [14].
- Even more interesting is the combination of the temperature-based metrics with the radiation parameters based on the bolometry tomographic inversion indicating core and off axis peaked radiation $P_{rad,core}$ and $P_{rad,out}$.
- In this case the combined temperature-radiation parameters provide in several cases earlier warning with respect to the stops wired in the JET control systems as shown in FIG. 7

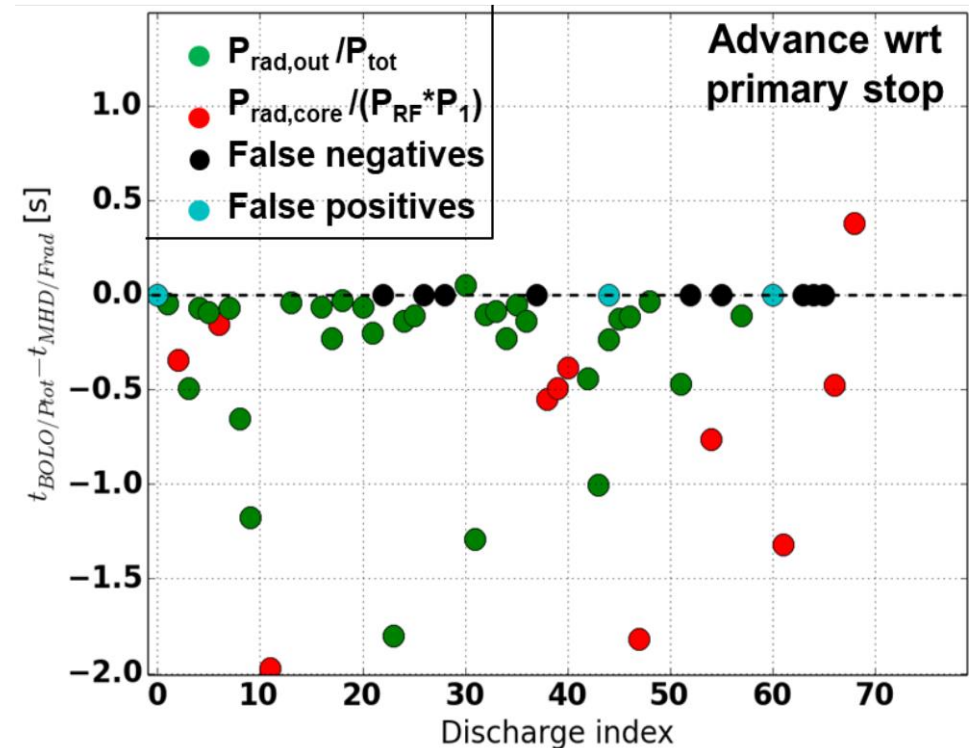


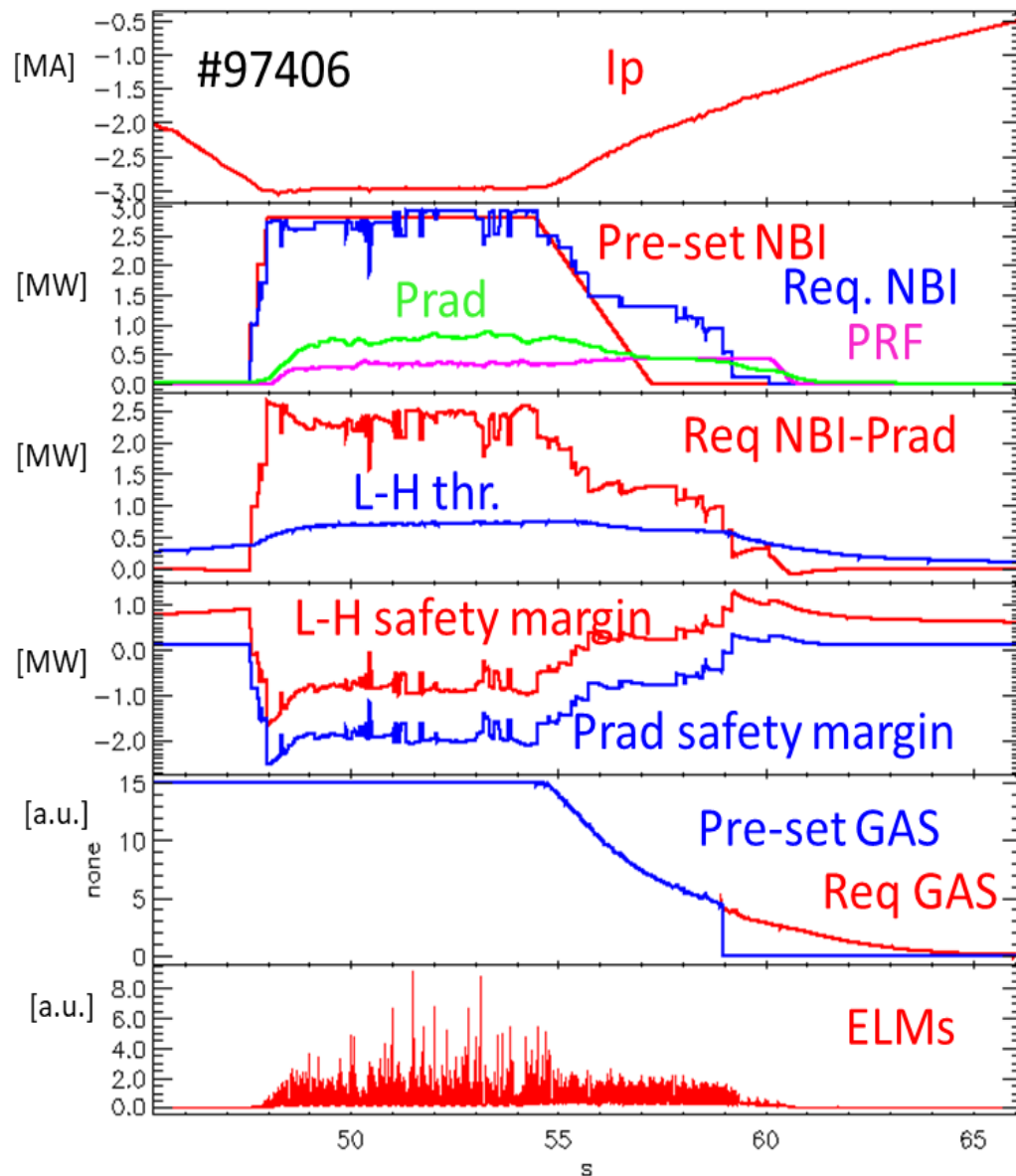
FIG. 7 Advance of the combined temperature-radiation metrics with respect to JET primary stop in the test database

5. TERMINATION ALGORITHM



- A termination algorithm inspired by Raptor simulations of JET and Asdex Upgrade ramp-down and aiming to optimize the input power waveform and the gas injection during the ramp-down in order to keep a safety margin to overcome the radiative losses both in H and L mode has been proposed, implemented and tested primarily for the application in baseline scenario termination [15][16] .
- It is motivated by the observation that some disruptions, particularly during the termination of higher field and plasma current pulses seem to be linked to the proximity of the H-L threshold and then prone to back-transitions into L mode leading to a pause in the ELMs activity and to the impurity accumulation that in turn further impacts the power balance.
- The algorithm gets the basic real time signals, computes the derived signals to obtain the real time power balance taking into account the operational limits such Greenwald density and H-L transition power and determines if the operational point is close to the danger limits. If this is the case it computes the additional power and the target gas flow and ELM frequency needed either to stay in H-mode or to safely ramp-down the pulse depending on the danger evaluation and on the pulse phase. An important part of the algorithm is also to control the power balance in L-mode avoiding the radiative collapse.

5. TERMINATION ALGORITHM



- FIG. 8 Example of a baseline plasma ramp-down controlled by the termination algorithm. Box 3 and 4 from top shows the computed power thresholds and the requested additional power also represented in box 2 with its feedforward waveform. The Pre-set gas in box 5 is the standard flow control following in real time current ramp-down. In this example the algorithm output for the gas request was already satisfied without further modifications.

5. TERMINATION ALGORITHM



- The algorithm has been successfully applied in several 3 MA flat top baseline cases as shown in FIG. 8. Its application at higher current is at present less reliable when the radiated power is already close to the maximum available power thus due to lack of actuator. Further developments aiming to improve the reliability of the input signals, the gas flow control and the evaluation of danger are being pursued. The algorithm has been successfully applied in the ITER baseline $q_{95}=3$ scenario at Asdex Upgrade [17].

6. CONCLUSIONS



- The development of safe termination schemes is part of the scenario preparation for the DT campaign in JET.
- A number of control-oriented elaboration schemes exploiting the diagnostics signals available in real time have been developed and tested particularly for the disruptive chains of events related with heavy impurities pollution.
- The low disruption rate reached for the hybrid scenario is already satisfactory.
- The margins of improvement of the disruption rate for the baseline scenario are still unclear particularly for higher plasma current.
- Important limitations on this respect appear related to the technical boundaries such the maximum available power and the need of maintaining a relatively short termination phase.



FEC 2020

28th IAEA Fusion Energy Conference



- [1] Suckewer S and Hawryluk R J 1978 Phys. Rev. Lett. 40 1649
- [2] C. Angioni, et al. et al 2014 Nucl. Fusion 54 083028
- [3] F Köchl et al 2018 Plasma Phys. Control. Fusion 60 074008
- [4] E. de la Luna et al. 2018 27th IAEA Fusion Energy Conference – IAEA CN-258, EX/2-1
- [5] L. Garzotti et al 2019 Nucl. Fusion 59 076037
- [6] J. Hobirk et al 2018 Nucl. Fusion 58 076027
- [7] G.Pucella et al. 2021 Nucl. Fusion 61 2021 046020
- [8] M. Lehnen et al 2011 Nucl. Fusion 51 123010
- [9] I Ivanova-Stanik et al., Plasma Phys. Control. Fusion 63 (2021) 035008
- [10] D. R. Ferreira et al 2021 Fusion Eng. Des. 164 112179
- [11] D.R. Ferreira et al., Fusion Science and Technology, 76:8, 901-911
- [12] S. Schmuck et al., Rev. Sci. Instrum. 87, 093506 (2016)
- [13] M. Fontana et al., Fusion Engineering and Design 161(2020) 111934
- [14] M. Fontana et al., IAEA T. M. on Disruptions (2020)
<https://conferences.iaea.org/event/217/contributions/16694/>
- [15] O. Sauter, S. Aleiferis, A. Pau, G. Marceca, C. Stuart et al., private communication (2019)
- [16] A A Teplukhina et al 2017 Plasma Phys. Control. Fusion 59 124004
- [17] O. Sauter et al., this conference, IAEA-CN-887
- [18] A. Pau et al 2019 Nucl. Fusion 59 106017
- [19] J. Vega et al 2020 Nucl. Fusion 60 026001
- [20] A. Murari et al 2020 Nucl. Fusion 60 056003
- [21] E. Aymerich et al 2021 Nucl. Fusion 61 036013
- [22] G.Sias et al., Fusion Engineering and Design 138(2019) 254-266